Molecular mechanisms regarding potassium bromate-induced cardiac hypertrophy without apoptosis in H9c2 cells

SHU-CHUN KUO[1,2], YINGXIAO LI[3,4], YUNG-ZE CHENG[5], WEI-JING LEE[5], JUEI-TANG CHENG[3,6] and KAI-CHUN CHENG[4]

[1]Department of Optometry, Chung Hwa University of Medical Technology, Tainan 7170; Departments of [2]Ophthalmology and [3]Medical Research, Chi-Mei Medical Center, Tainan 71003, Taiwan R.O.C.; [4]Department of Psychosomatic Internal Medicine, Kagoshima University Graduate School of Medical and Dental Sciences, Kagoshima 890, Japan; [5]Department of Emergency Medicine, Chi-Mei Medical Center, Tainan 71003; [6]Graduate School of Medical Science, Chang Jung Christian University, Tainan 71101, Taiwan, R.O.C.

Received April 25, 2018; Accepted August 16, 2018

DOI: 10.3892/mmr.2018.9470

Abstract. Cardiac hypertrophy is commonly involved in cardiac injury. Oxidative stress can induce cardiac hypertrophy with apoptosis. Potassium bromate (KBrO3) has been widely used as a food additive due to its oxidizing properties. In the present study, the rat-derived heart cell line H9c2 was used to investigate the effect of KBrO3 on cell size. KBrO3 increased cell size at concentrations <250 μM, in a dose-dependent manner. Additionally, KBrO3 also promoted the gene expression of two biomarkers of cardiac hypertrophy, brain/B-type natriuretic peptides (BNP) and β-Myosin Heavy Chain (β-MHC). However, apoptosis remained unobserved in these cells. Moreover, mediation of free radicals was investigated using a fluorescence assay, and it was observed that superoxide and reactive oxygen species (ROS) levels increased with KBrO3. Effects of KBrO3 were significantly reduced by tiron at concentrations sufficient to produce antioxidant-like action. Additionally, signals involved in cardiac hypertrophy such as calcineurin and nuclear factor of activated T-cells (NFAT) were also determined using western blot analysis. KBrO3 increased the protein levels of both these molecules which were decreased by tiron in a dose-dependent manner. Additionally, cyclosporine A attenuated the cardiac hypertrophy induced by KBrO3 in H9c2 cells at concentrations effective to inhibit calcineurin, in addition to reducing mRNA levels of BNP or β-MHC. Finally, apoptosis was also identified in H9c2 cells incubated with KBrO3 at concentrations >300 μM. Collectively, these results provided a novel perspective that KBrO3 induces cardiac hypertrophy without apoptosis at a low dose through the generation of ROS, activating the calcineurin/NFAT signaling pathway in H9c2 cells. Therefore, at a dose <250 μM, KBrO3 can be applied as an inducer of cardiac hypertrophy without apoptosis in H9c2 cells. KBrO3 can also be developed as a tool to induce cardiac hypertrophy in animals.

Correspondence to: Professor Juei-Tang Cheng, Department of Medical Research, Chi-Mei Medical Center, 901 Zhonghua Road, Yong Kang, Tainan 71003, Taiwan, R.O.C.
E-mail: jtcheng5503@gmail.com

Dr Kai-Chun Cheng, Department of Psychosomatic Internal Medicine, Kagoshima University Graduate School of Medical and Dental Sciences, 8-35-1, Sakuragaoka, Kagoshima 890, Japan
E-mail: kc-cheng@m3.kufm.kagoshima-u.ac.jp

Abbreviations: BNP, brain/B-type natriuretic peptides; NFAT, nuclear factor of activated T-cells; ROS, reactive oxygen species

Key words: potassium bromate, oxidative stress, tiron, hypertrophic signals, H9c2 cells

Introduction

Cardiac hypertrophy, the first phase of cardiovascular disease, induces heart failure. However, cardiac hypertrophy is an important compensatory mechanism in response to physiological or pathological stimuli that involve regulation of cellular signaling mediators and transcript factors (1-3). Hypertrophic signals result in increased protein synthesis and increased cell cycle (4). Cardiac hypertrophy is characterized by cell enlargement, involving physiological and pathological hypertrophy (5). Pathological cardiac hypertrophy is often coupled with interstitial and perivascular fibrosis, in addition to apoptosis and the release of atrial natriuretic peptides (ANP) and brain/B-type natriuretic peptides (BNP). With the initiation of cardiac hypertrophy, concentric hypertrophy is the primary phenotype that highly resists after-load and is known as the adaptive phase. As the cardiac damage progresses, cell length increases, leading to increased hypertrophy (6). In cardiac hypertrophy, nuclear factor of activated T-cells (NFAT) is considered an important mediator of several signal-transduction pathways involved in the coordination of pathological stimulation (7). The role of reactive oxygen species (ROS) in the induction of cardiac hypertrophy has been demonstrated (8). However, oxidative stress induces apoptosis in addition to cardiac hypertrophy (9). Therefore, the development of a model of cardiac hypertrophy only without apoptosis is essential.

Potassium bromate (KBrO3) has been widely used as a food additive and is also a by-product of disinfecting drinking water by ozonization (10). KBrO3 is applied primarily due to its oxidizing properties and may cause lipid peroxidation and oxidative DNA damage in humans and other mammals (11). KBrO3 is also known as a rodent carcinogen (12,13) and as a renal and/or neuro-toxicant in humans (14).

Free radicals produced by KBrO3 are easily associated with cardiac injury, as the heart is very sensitive to ROS-induced damage (15). Thus, KBrO3 has been classified as one of the cardiac toxins because lipid peroxidation increases with a significant reduction in cardiac antioxidant capacity (16). Recently, vanillin has been demonstrated as an antioxidant as it improves KBrO3-induced cardiac injury in mice (17). However, the effect of KBrO3 on cardiac hypertrophy remains undetermined.

In the present study, KBrO3 was applied to the cardiac cell line H9c2, which is widely used to induce cardiac hypertrophy (18). The aim was to develop a novel and simple model of cardiac hypertrophy without apoptosis *in vitro*.

Materials and methods

Materials. Potassium bromate (KBrO3), cyclosporine A, and antioxidant (tiron) were purchased from Sigma-Aldrich (Merck KGaA, Darmstadt, Germany). All other reagents were obtained from the supplier as indicated and were at least of analytical grade.

Cell culture. The H9c2 cells (cat. no. 60096; Bioresource Collection and Research Center, Hsinchu, Taiwan) were cultured as previously described (19). In brief, H9c2 cells were maintained in Dulbecco's modified Eagle's medium (pH 7.2; Gibco; Thermo Fisher Scientific, Inc., Waltham, MA, USA) supplemented with 10% fetal bovine serum (GE Healthcare Life Sciences, Little Chalfont, UK). The H9c2 cells were plated at a density of 6,000 cells/cm^2 and were allowed to proliferate in the growth medium. Following plating, the medium was replaced on the second day. The next day, cells were incubated with testing agent(s) as described below.

Experimental protocol. Briefly, H9c2 cells were incubated with KBrO3 to identify the changes in cell size. Then, inhibitor was used to pretreat at 37˚C for 60 min prior to the addition of KBrO3. Solvent applied to dissolve the inhibitor was also pretreated in same manner at same volume and was termed the vehicle-treated group. Specific inhibitor(s) were applied to investigate the potential mechanism(s) of KBrO3. Cyclosporine A (CsA) is a powerful immunosuppressant and has also been used to inhibit calcineurin (20). Therefore, as previously reported (21), CsA at an effective concentration (500 nM) was incubated with H9c2 cells at 37˚C for 1 h prior to the treatment with KBrO3. Additionally, tiron is a water-soluble and cell permeable antioxidant that scavenges superoxide (22,23). It was also applied as detailed above for CsA to investigate the role of free radicals in the effects of KBrO3.

Measurement of cardiac hypertrophy. H9c2 cells at a density of 7.5x10^3 cells/ml were arranged on a 24-well plate (Greiner Bio-One, Monroe, North Carolina, USA). Cells were starved for 4 h in a serum-free medium prior to treatment with KBrO3 at 37˚C for 72 h. Briefly, following washing twice with cold PBS, the cells were fixed in 4% paraformaldehyde at room temperature for 15 min and washed with PBS containing 2% bovine serum albumin (GE Health Care Life Sciences) and 0.1% Triton X-100. Cells were stained with rhodamine phalloidin (Invitrogen; Thermo Fisher Scientific, Inc.) for 25 min at room temperature to identify the actin filaments and with DAPI (Abcam, Cambridge, UK) to stain the nucleus. An entire field of vision was characterized using a fluorescence microscope (IX71; Olympus Corporation, Tokyo, Japan) connected to an imaging system (DP2-BSW; Olympus Corporation). The cell sizes were magnified x200 and analyzed by the imaging system. Cell surface area size was determined and quantified by imaging to the complete boundary of the individual cells. The results were subsequently expressed as the percentage change of the surface area level of the cells, based on analysis using image J program, version 1.46 (National Institutes of Health, Bethesda, MD, USA; http://imagej.nih.gov/ij/) as described previously (24).

Identification of intracellular superoxide levels. Following the methods described in a previous study (25), H9c2 cells were seeded in 24-well plates at a density of 7.5x10^3 cells/ml at 37˚C overnight. Following starvation for 4 h in a serum-free medium, the cells were treated with 250 μM KBrO3 at 37˚C for an additional 72 h. For the detection of the intracellular superoxide levels, dihydroergotamine (10 μM) from Thermo Fisher Scientific Inc. was applied to react with intracellular superoxide ions at 37˚C for 30 min following treatment with KBrO3. An entire field of vision was characterized using a fluorescence microscope (IX71, Olympus Corporation) connected to an imaging system (DP2-BSW, Olympus Corporation). The results were subsequently expressed as a percentage of the intracellular superoxide levels in the cells based on the analysis using image J program, version 1.46 (National Institutes of Health), as described previously (24).

Determination of intracellular calcium. Changes in the intracellular calcium concentrations were also detected using a fluorescent probe, fura-2, as described previously (26). Fluorescence was continuously recorded by a fluorescence spectrofluorometer (F-2000; Hitachi, Ltd., Tokyo, Japan). The values of [Ca^{2+}]i were determined as described previously (26).

Reverse-transcription-quantitative polymerase chain reaction (RT-qPCR). As previously described (24), Total RNA was extracted from H9c2 cells using TRIzol reagent (Life Technologies; Thermo Fisher Scientific, Inc.). Total RNA (5 μg) was reverse-transcribed into cDNA with random hexamer primers (Roche Diagnostics GmbH, Mannheim, Germany). Analysis was carried out using LightCycler (Roche Diagnostics GmbH). PCR cycles were under the following conditions: Pretreatment at 95˚C for 10 sec, 96˚C for 10 sec, 60˚C for 30 sec, 72˚C for 1 sec, 40˚C for 30 sec (45 cycles). β-actin was used as the control of the input RNA level. The primers used in RT-qPCR analysis were designed by Roche (Roche Diagnostics GmbH). The concentration of each PCR product was calculated relative to a corresponding standard curve. Analysis of relative gene expression data using

real-time quantitative PCR and the $2^{-\Delta\Delta Cq}$ method as described previously (27). The relative gene expression was subsequently indicated as the ratio of the target gene level to that of β-actin. The primers for BNP, β-Myosin Heavy Chain (β-MHC), and β-actin were:

BNP forward, 5'-GTCAGTCGCTTGGGCTGT-3' and reverse, 5'-CCAGAGCTGGGGAAAGAAG-3';β-MHC forward, 5'-CATCCCCAATGAGACGAAGT-3' and reverse, 5'-GGG AAGCCCTTCCTACAGAT-3'; β-actin forward, 5'-CTAAGG CCAACCGTGAAAAG-3' and reverse, 5'-GCCTGGATG GCTACGTACA-3'.

Western blot analysis. Cells were harvested and washed with ice cold phosphate buffer solution, then homogenized in radio immunoprecipitation assay buffer which was prepared according to a previous method (24). Lysates were mixed and incubated on ice for 10 min. Cell debris was precipitated at 4˚C for 10 min (16,099 x g). Protein concentrations were measured by bicinchoninic acid protein assay (Thermo Fisher Scientific, Inc.). Proteins were separated by 10% or 15% SDS-PAGE and electro-transferred onto a polyvinylidene fluoride membrane. Nonspecific binding was blocked by incubation in 5% nonfat milk at room temperature for 2 h. Membranes were subsequently incubated with the primary antibodies (at 1:1,000 dilution) at 4˚C overnight, washed 3 times with TBST (0.05% Tween-20) and finally incubated with a HRP-conjugated secondary antibody at room temperature for 1 h. Protein bands were visualized using an chemiluminescence (ECL) kit (PerkinElmer, Inc., Waltham, MA, USA). The optical densities of the bands for calcineurin (18 kDa), NFAT3 (100 kDa), Histone H3 (15 kDa), and β-actin (43 kDa) were quantified using a laser densitometer (CHEM-400; Avegene Life Science, Taipei, Taiwan), as described in a previous study (28). The target antigens from the protein extracts were detected using primary antibodies specific for calcineurin (C0581; Sigma-Aldrich; Merck KGaA), NFAT3 (PA-1-021; Thermo Fisher Scientific, Inc.), or β-actin (A5441; Sigma-Aldrich; Merck KGaA) and Histone H3 (SC-8654; Cell Signaling Technology, Inc., Danvers, MA, USA). Additionally, the apoptotic markers such as Bcl2 (AB59348; Abcam, Cambridge, MA, USA), AIF (07-208; Merck KGaA) and Caspase-3 (9662S; Cell Signaling Technology, Inc.) were also determined.

Nuclear extraction. The extraction of the nuclear fraction was performed according to a previously described method (28), using a CNMCS Compartmental Protein Extraction Kit (BioChain Institute, Inc., Hayward, CA, USA). Briefly, H9c2 cells were collected and ice-cold lysis buffer (2 ml per 20 million cells) added to them. The cell mixture was passed through the needle base 50-90 times to disrupt the cell membranes and to release the nuclei from the cells. The degree of cell membrane disruption and the release of nuclei were monitored with a fluorescence microscope. The mixture was then centrifuged at 15,000 x g at 4˚C for 20 min. The supernatant, which contained cytoplasmic proteins, was removed and was saved in a separate tube. The pellet was resuspended in ice-cold washing buffer (4 ml per 20 million cells), and the suspension was rotated at 4˚C for 5 min, followed by centrifugation at 15,000 x g at 4˚C for 20 min. The supernatant was removed and ice-cold nuclear extraction buffer (1 ml per 20 million cells) was added to the pellet. Following rotation at 4˚C for 20 min, the suspension was centrifuged at 15,000 x g at 4˚C for 20 min. The supernatant, which contained nuclear proteins, was removed and saved for further use.

Cytotoxicity assay. Cell viability and survival were determined by an MTT assay (29). Briefly, 5,000 cells were plated in 24-well plates in triplicate and treated with concentrations between 250 and 5,000 μM of KBrO3 at 37˚C for 72 h. Following treatment, the medium was removed and replaced with 500 μl/well fresh medium, and 50 μl MTT (final concentration 0.5 mg/ml) was added to each well. The plates were incubated at 37˚C for 4 h, allowing viable cells to reduce the yellow tetrazolium salt into dark blue formazan crystals. The formazan crystals were dissolved using a solution of 0.01 M HCl/SDS 10%. Finally, the absorbance in each individual well was determined at a wavelength of 595 nm, with the absorbance of the cells counted by a Synergy HT Multi-Mode Microplate Reader (BioTek Instruments, Inc., Winooski, VT, USA). Relative cell viabilities were calculated as percentages vs. control cells: Relative cell viability (%)=(absorbance of treated cells)/(absorbance of control cells) x100%.

Staining of live and dead cells. To image the live and dead cells, a LIVE/DEAD viability assay kit (Molecular Probes; Thermo Fisher Scientific, Inc.) was used, according to the manufacturer's protocol. H9c2 cells at a density of $5x10^4$ cells/ml were incubated with two probes, calcein-AM (green color) and ethidium homodimer-1 (EtdD-1, bright red color), for intracellular esterase activity and plasma membrane integrity, respectively. Subsequently, specimens were observed under a fluorescence microscope (Olympus IX71; Olympus Corporation). The live cells are shown in green and the dead cells in red (magnification, x4). The images were analyzed using image J program, version 1.46 (National Institutes of Health). Each assay performed in triplicate.

Flow cytometry analysis. H9c2 apoptotic cell measurement was performed by flow cytometry with Annexin V-propidium iodide staining, as described previously (30), using a fluorescein isothiocyanate (FITC) Apoptosis Detection Kit (BD Biosciences, San Diego, CA, USA). The Annexin reagent utilizes Annexin V to detect phophatiylserine of apoptotic cells and a dead cell marker as an indicator of membrane stability. H9c2 cells were seeded in a dish (10 cm) at a density of $1x10^6$ cells/well, and the experimental procedure was performed according to the manufacturer's protocol. Staining was analyzed by fluorescence-activated cell sorting on a flow cytometer (NOVO Cyte 3000; ACEA Biosciences, San Diego, CA., USA). Spectral compensation and data quantification were performed using NovoExpress software (2017 Version; ACEA Biosciences Inc., San Diego, CA, USA) that provided a variety of plots and gates for flow cytometry data analysis.

Statistical analysis. Data are presented as the mean ± standard error from the indicated sample size (N) eachperformed in triplicate. One-way analysis of variance withpost hoc Tukey test was used for multiple comparisons by SPSS

Table I. Effects of KBrO3 on cultured cardiac cells.

Contents	Control	KBrO3 (100 μM)	KBrO3 (200 μM)	KBrO3 (250 μM)
Relative area level (fold change)	1.00±0.07	1.46±0.06	2.07±0.11[a]	2.74±0.09[b]
Relative mRNA level of BNP/β-Actin	1.00±0.00	1.19±0.03	1.60±0.05[a]	2.09±0.07[b]
Relative mRNA levels of β-MHC/β-Actin	1.00±0.00	1.13±0.05	1.54±0.05[a]	1.99±0.01[b]
Ratio of Bcl2/β-Actin protein	0.74±0.08	0.74±0.09	0.73±0.09	0.73±0.07
Ratio of Caspase-3/β-Actin protein	0.63±0.09	0.62±0.08	0.61±0.07	0.60±0.07
Ratio of AIF/β-Actin protein	0.70±0.10	0.70±0.09	0.67±0.08	0.68±0.08

Data are presented as the mean ± standard error (n=6). [a]P<0.05 or [b]P<001 vs. the non-treated control. AIF, apoptosis-inducing factor; Bcl, B-cell lymphoma; β-MHC, β-Myosin Heavy Chain; BNP, brain/Btype natriuretic peptides; KBrO3, potassium bromate.

version 16.0 software (SPSS, Inc., Chicago, IL, USA). P<0.05 was considered to indicate a statistically significant difference.

Results

Effect of KBrO3 on H9c2 cell size. In a preliminary experiment, H9c2 cells were incubated with KBrO3 (150 μM) for 24, 48, 72 and 84 h. KBrO3 increased the H9c2 cell size gradually, with the maximal response observed at 72 h following treatment (data not shown). Therefore, H9c2 cells were incubated with KBrO3 at concentrations of 150 μM for 72 h. However, different from high glucose, cellular osmolarity was not influenced by KBrO3 in the preliminary experiments. As demonstrated in Fig. 1A, KBrO3 increased the H9c2 cell size in a dose-dependent manner as shown in Table I. Additionally, the mRNA expression levels of the biomarkers of cardiac hypertrophy, such as BNP and β-MHC were also increased by KBrO3 in the same manner, as demonstrated in Table I. However, KBrO3 did not modify the cell number of H9c2 cells even at the highest dose (control group: $8.2x10^4$ cells/cm^2; KBrO3 250 μM group: $7.8x10^4$ cells/cm^2). Notably, apoptosis was not identified in H9c2 cells incubated with KBrO3 at the effective concentrations as demonstrated in Fig. 1B and Table I as the levels of apoptosis-associated markers remain unchanged.

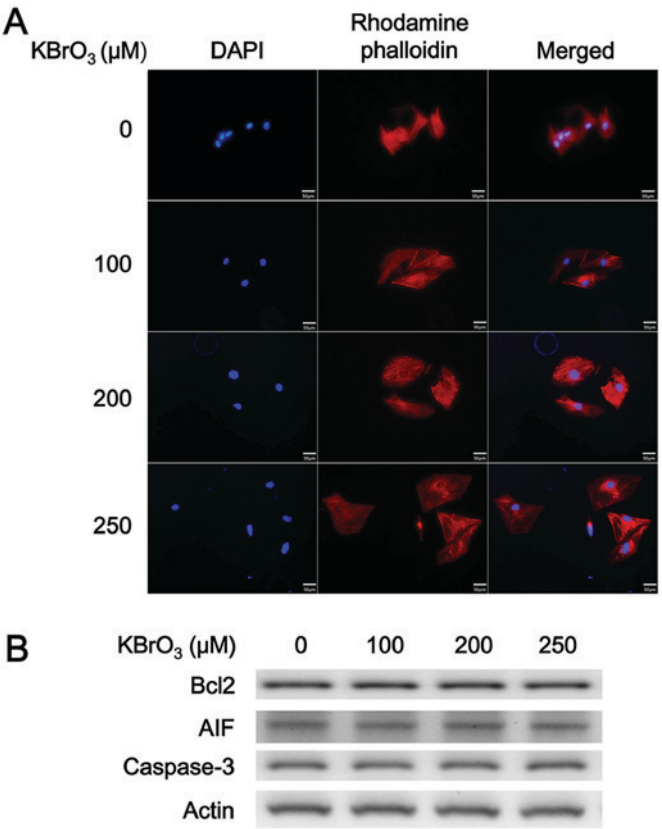

Figure 1. Effects of KBrO3 on the cardiac cell line H9c2. Cells incubated with KBrO3 at the indicated concentrations were used to assay (A) cell size and (B) changes in levels of various proteins associated with apoptosis. AIF, apoptosis-inducing factor; Bcl2, B-cell lymphoma; KBrO3, potassium bromate.

Oxidative stress and KBrO3-induced cardiac hypertrophy in H9c2 cells. The changes in two oxidative biomarkers, ROS and superoxide, were investigated following KBrO3-induced cardiac hypertrophy in H9c2 cells. As demonstrated in Fig. 2, KBrO3 notably increased levels of both oxidative biomarkers, and these were reversed by tiron at effective concentrations.

Effect of antioxidant on KBrO3-induced cardiac hypertrophy in H9c2 cells. H9c2 cells were treated with the antioxidant tiron to investigate the mediation of oxidative stress following the KBrO3-induced cardiac hypertrophy. Following pretreatment with tiron for 30 min, cardiac hypertrophy induced by KBrO3 was reduced in a dose dependent manner (Fig. 3A). Additionally, the expression levels of the two biomarkers BNP and β-MHC were also similarly reduced by tiron, as demonstrated in Table II.

Cellular signaling pathway and KBrO3-induced cardiac hypertrophy in H9c2 cells. Cardiac hypertrophy is controlled simultaneously by stimulatory (prohypertrophic) and counter-regulatory (antihypertrophic) mechanisms via the calcineurin-NFAT signaling pathway (31). Therefore, the changes in the signaling pathway were investigated using western blotting. As demonstrated in Fig. 3, both calcineurin (Fig. 3B) and NFAT3 expression (Fig. 3C) levels were elevated by KBrO3 at the concentration sufficient to induce cardiac hypertrophy in H9c2 cells. However, this action of KBrO3 was

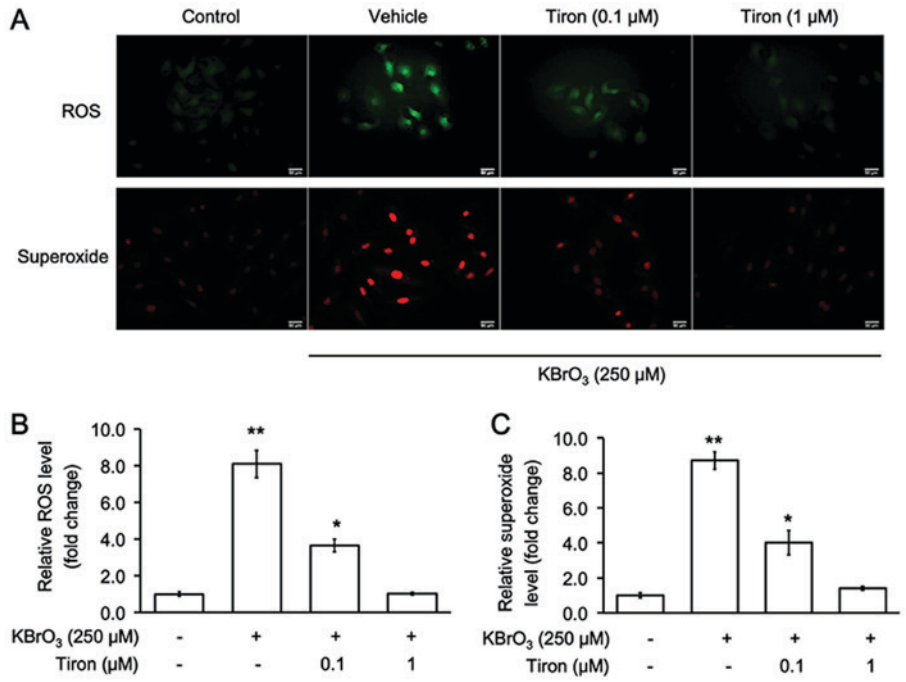

Figure 2. Free radicals induced by KBrO3 in H9c2 cells. (A) Representative images demonstrating the formation of free radicals, such as ROS and superoxide, induced by KBrO3 at the indicated concentration. The antioxidant tiron at the indicated concentrations reduced the effect of KBrO3 in a dose dependent manner, compared with the vehicle-treated control (vehicle was the solvent used to dissolve tiron). (B) Quantification of ROS and (C) quantification of superoxide levels. Data are presented as the mean ± standard error (n=6). *P<0.05 or **P<0.01 vs. the non-treated control. KBrO3, potassium bromate; ROS, reactive oxygen species.

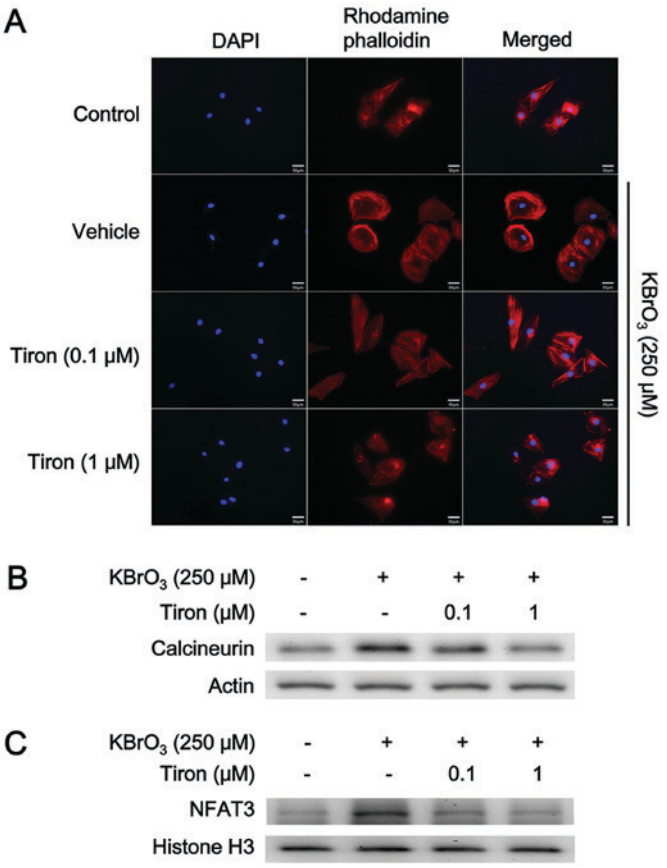

Figure 3. The antioxidant tiron attenuates KBrO3-induced cardiac hypertrophy in H9c2 cells. Cells incubated with KBrO3 at the indicated concentration were used to investigate (A) the cell size and the changes in hypertrophic signals, such as (B) calcineurin and (C) NFAT3.KBrO3, potassium bromate; NFAT3, nuclear factor of activated T-cells.

reduced by tiron in a dose dependent manner (Fig. 3B and C; Table II). Moreover, the cellular calcium levels were measured and it was demonstrated that KBrO3 increased cellular calcium levels which were then attenuated by tiron, as demonstrated in Table II.

Cyclosporine A inhibits KBrO3-induced cardiac hypertrophy in H9c2 cells. Cyclosporine A (CsA) is a powerful immunosuppressant and has also been used to inhibit calcineurin (20). The cell size of H9c2 and mRNA expression levels of BNP and β-MHC were measured. As illustrated in Fig. 4, CsA inhibited KBrO3-induced cardiac hypertrophy in H9c2 cells. Therefore, mediation of the calcineurin-NFAT signaling pathway in KBrO3-induced cardiac hypertrophy was identified.

Characterization of KBrO3-induced apoptosis and damage in H9c2 cells. In a previous study, apoptosis was induced by H_2O_2 at concentrations higher than that used to induce cardiac hypertrophy in cardiac cells (32). Therefore, the possible toxic effect of KBrO3 on H9c2 cells was investigated. As demonstrated in Fig. 5A, KBrO3 at high concentrations may damage H9c2 cells and cell death was observed in H9c2 cells treated with KBrO3 >1 mM, in a dose-dependent manner. Epifluorescent staining of cells following treatment with KBrO3 illustrated mostly apoptotic/necrotic cells with orange red fluorescent nuclei (Fig. 5B) while cells with green fluorescent nuclei were considered as an indicator of live cells, indicating that cells underwent apoptosis at high doses of KBrO3. Additionally, Annexin V-FITC staining was used. As demonstrated in Fig. 5C and D, apoptosis induced by KBrO3 at high doses was clearly identified using the flow cytometry.

Table II. Cardiac hypertrophy induced by KBrO3 is reduced by the antioxidant Tiron.

Contents	Control	Vehicle + $KBrO_3$ (250 μM)	Tiron (0.1 μM) + $KBrO_3$ (250 μM)	Tiron (1 μM) + $KBrO_3$ (250 μM)
Relative area level (fold change)	1.00±0.08	2.56±0.12[b]	1.62±0.10[a]	1.02±0.09
Relative mRNA level of BNP/β-Actin	1.00±0.00	1.96±0.04[b]	1.48±0.03[a]	1.22±0.05
Relative mRNA level of β-MHC/β-Actin	1.00±0.00	1.91±0.06[b]	1.49±0.05[a]	1.20±0.04
$[Ca^{2+}]$nM	176.30±4.06	327.40±11.22[b]	257.32±13.28[a]	185.69±9.58
Ratio of calcineurin/β-Actin protein	0.31±0.04	0.81±0.05[b]	0.49±0.04[a]	0.29±0.03
Ratio of NFAT3/Histone H3 protein	0.45±0.02	0.87±0.05[b]	0.63±0.02[a]	0.49±0.04

Data are presented as the mean ± standard error (n=6) (Vehicle the solvent used to dissolve tiron). [a]P<0.05 or [b]P<0.01 vs. the non-treated control. β-MHC, β-Myosin Heavy Chain; BNP, brain/Btype natriuretic peptides; KBrO3, potassium bromate.

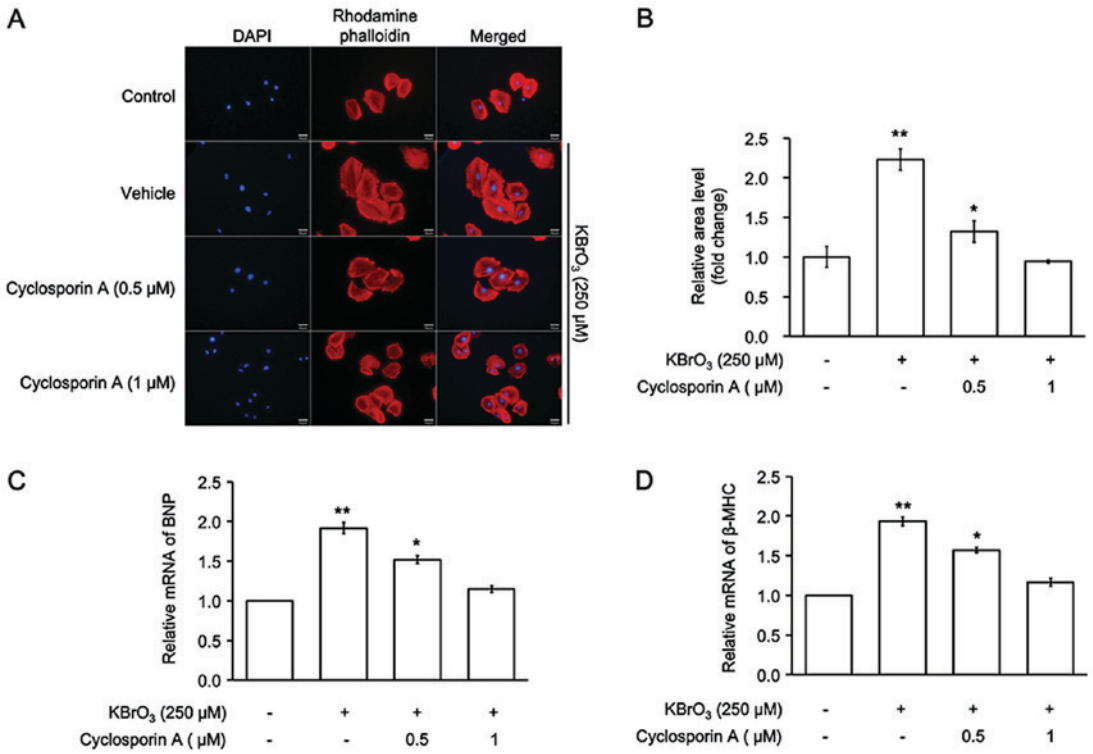

Figure 4. Cyclosporine A, a calcineurin inhibitor, attenuates KBrO3-induced cardiac hypertrophy in H9c2 cells. Cells incubated with KBrO3 were used to investigate cardiac hypertrophy, via (A and B) cell size changes and the mRNA expression levels of the hypertrophic indicators, such as (C) BNP and (D) β-MHC (Vehicle was the solvent used to dissolve cyclosporine A). Data are presented as the mean ± standard error (n=6). *P<0.05 or **P<0.01 vs. the non-treated control. β-MHC, β-Myosin Heavy Chain; BNP, brain/B-type natriuretic peptides; KBrO3, potassium bromate.

Discussion

In the present study, KBrO3 at concentrations <250 μM induced cardiac hypertrophy without apoptosis in a cultured cell line. Additionally, it was demonstrated that free radicals and/or oxidative stress were mediated by the effect of KBrO3, which is fully consistent with previous reports that KBrO3 induces damage via oxidative stress (10-12). Cardiac injury induced by KBrO3 has also been observed in rats (15,16), and histological evidence demonstrates that KBrO3 induces cardiac apoptosis and/or necrosis in rodents (33). However, cardiac hypertrophy induced by KBrO3 has not been previously examined.

The direct effect of KBrO3 on cardiac cells resulted in an increase in the size of H9c2 cells, which was demonstrated using visual identification and a parallel increase in biomarkers of cardiac hypertrophy. Increased expression levels of ANP or BNP in plasma levels are widely used as reliable indicators of cardiac hypertrophy in the clinic (34). In the present study, the mRNA expression level of BNP in H9c2 cells was increased by KBrO3 in a dose-dependent manner. This was in addition to another indicator β-MHC, which has been described previously (35). Similar to natriuretic peptides, β-MHC or α-skeletal actin has also been used as a biomarker of pathological hypertrophy (36). In the present study, KBrO3, similar to its role in increasing the expression of BNP, also increased the expression of β-MHC. Furthermore, KBrO3 increased the size of H9c2 cells (hypertrophy) but did not increase cell numbers (hyperplasia).

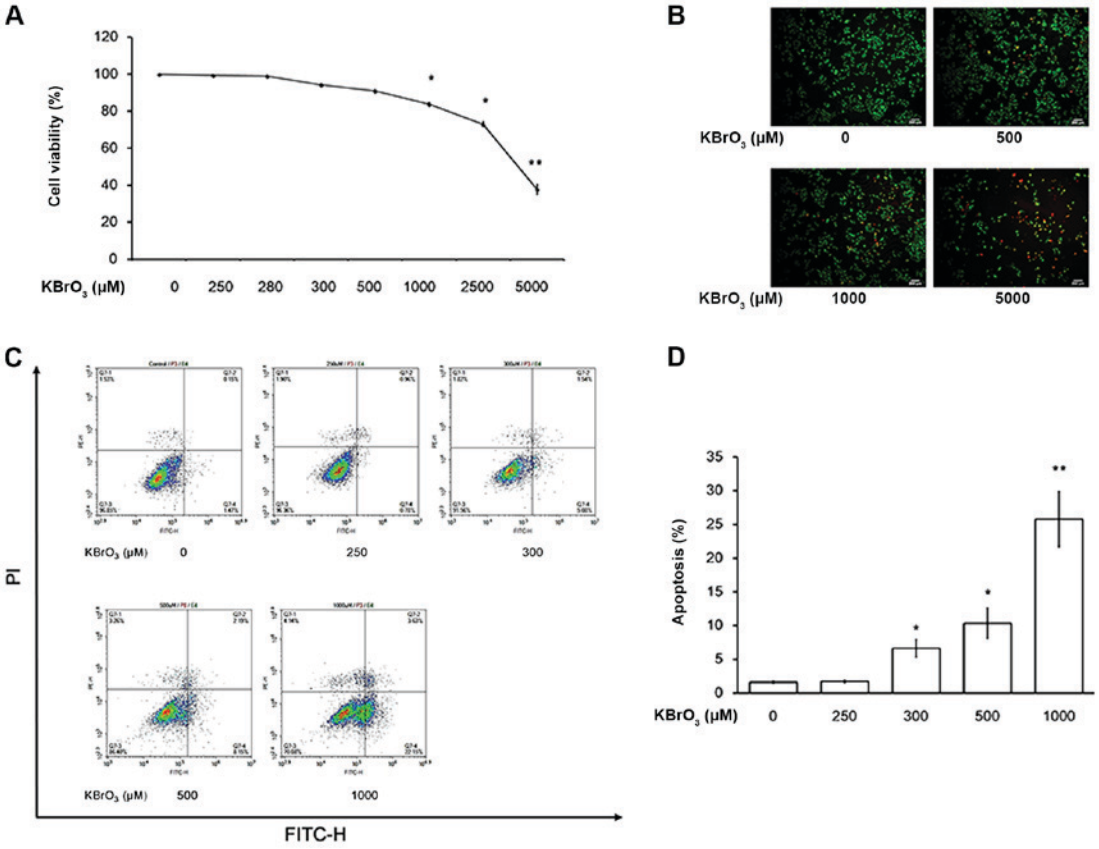

Figure 5. Cell death is induced by KBrO3 at high concentrations in H9c2 cells. (A) KBrO3 damaged cardiac cells at concentrations >1 mM. (B) Cell death measured using a LIVE/DEAD viability assay kit. (C) Apoptosis was measured by Annexin V-FITC analysis and (D) its quantification indicated that apoptosis occurred in H9c2 cells incubated with KBrO3 at concentrations >300 μM. *P<0.05 or **P<0.01 vs. the non-treated control (at dose 0). KBrO3, potassium bromate; FITC, fluorescein isothiocyanate; PI, propidium iodide.

Therefore, KBrO3 induced cardiac hypertrophy in H9c2 cells.

ROS produced by KBrO3 are proposed as the primary mediators in tissue damage (11,16). Thus, the changes in ROS and superoxide levels were investigated. Similar to hyperglycemia-induced cardiac damage (24), KBrO3 increased ROS and superoxide levels in H9c2 cells. Additionally, the effect of tiron, which is a water-soluble and cell permeable antioxidant that scavenges superoxide (22,23), reduced the effect of KBrO3 in a dose-dependent manner. Tiron alleviates cardiac damage through a marked reduction in oxidative stress (37,38). In the present study, tiron inhibited the effects of KBrO3 including the induction of cardiac hypertrophy and formation of ROS in H9c2 cells.

H_2O_2 induces cardiac hypertrophy only at concentrations <50 μM in cardiomyocytes isolated from rats (32). Furthermore, KBrO3 induced disorder at concentrations <250 μM in the cultured H9c2 cell line. Similar to the effects of H_2O_2, KBrO3 induced apoptosis and/or necrosis in H9c2 cells at high concentrations (>300 μM). Therefore, the effective concentration of KBrO3 is limited within this range for the induction of cardiac hypertrophy in H9c2 cells.

The role of the calcineurin signaling pathway was also investigated in KBrO3-induced cardiac hypertrophy. Calcineurin may dephosphorylate NFAT3, leading to nuclear translocation (31). Subsequently, the nuclear NFAT3 participates in the promotion of hypertrophic gene expression including that of BNP and β-MHC to induce cardiac hypertrophy (6,7). Additionally, ROS increases cellular calcium (39). In the present study, it was demonstrated that KBrO3 significantly increased the calcium level, which may promote the calcineurin and NFAT3 signaling pathway in H9c2 cells. This conclusion is also supported by the evidence from cyclosporine A, which at a concentration effective to inhibit calcineurin, attenuated the KBrO3-induced cardiac hypertrophy. Notably, these effects of KBrO3 were also reduced by tiron in a dose-dependent manner. Therefore, KBrO3 likely increases hypertrophic signaling via elevation of ROS in H9c2 cells, but this needs to investigate in the future.

The mechanism(s) for oxidative stress-induced cardiac hypertrophy remains unclear. Many parameters have been examined (40), including osteopontin (41). However, most of these reports have investigated hyperglycemia-induced cardiac damage, particularly apoptosis (40). Hyperglycemia induces cardiac injury primarily through ROS generation (38). However, the inflammatory parameters are also involved in diabetic cardiomyopathy, particularly in the *in vivo* models (42). Therefore, the difference in cardiac hypertrophy between hyperglycemia and KBrO3 should be clarified in the future.

In cardiac research, oxidative stress or ROS-induced cardiac hypertrophy is widely induced by H_2O_2 in H9c2 cells (43). Additionally, 4-hydroxy-2-nonenal (44) or lactosylceramide (45) has also been applied to induce cardiac hypertrophy via ROS in a way similar to that of KBrO3.

Therefore, KBrO3 could be used as an inducer of cardiac hypertrophy in cells. In rats, KBrO3 at a dose of 1.2 g/kg for 4 weeks produces damages without mortality (46), and in Sprague-Dawley rats, KBrO3 at a dose of 20 mg/kg for 4 weeks induces cardiac injury (47). Generally, KBrO3 at a dose of 20-30 mg/kg damages cardiac tissues in rats (16). The histological evidence also demonstrates that KBrO3 at 20 mg/kg twice weekly for 4 weeks induces cardiac fibrosis in rats (33). In a clinic, nine cases of accidental KBrO3 poisoning in a bakery demonstrated hematemesis and renal failure as the possible adverse outcomes (48). Although the cardiac injury seems not so critical in the human response to KBrO3, further investigations on human cardiac cells are required. Moreover, characterization of the dose of KBrO3 effective to induce cardiac hypertrophy in animals is also essential in the future. The role of signaling pathways need to be investigated using small interfering or short hairpin RNA techniques, in order to understand the damage resulting from KBrO3 in cardiomyocytes. Additionally, the effects of potassium or bromate on cardiac hypertrophy remain unclear. Further investigations are required to evaluate the pharmacokinetics and/or pharmacodynamics of KBrO3.

In conclusion, in the present study, KBrO3 at concentrations <250 μM induced cardiac hypertrophy in H9c2 cells without apoptosis mainly through free radicals to increase cellular calcium levels and so activate the calcineurin and NFAT3 signaling pathway. Therefore, KBrO3 may be applied to develop a novel cell model of cardiac hypertrophy for future research.

Acknowledgements

Authors would like to thank Miss Yang-Lien Yen and Mr. Yi-Zhi Chen for their assistance in the experiments.

Funding

The present study was partly supported by a grant (grant no. CMFHT10503) from Chi-Mei Medical Center, Yong Kang, Tainan City, Taiwan.

Availability of data and materials

The datasets used and analyzed during the present study are available from corresponding author on reasonable request.

Author's contributions

SK, KC and JC designed experiments. YL, YC and WL performed the experiments and analyzed data. SK, YL and KC drafted the manuscript. All authors discussed, revised, and approved the manuscript.

Ethics approval and consent to participate

Not applicable.

Patient consent for publication

Not applicable.

Competing interests

The authors declare that they do not have any competing interests.

References

1. Frey N, Katus HA, Olson EN and Hill JA: Hypertrophy of the heart: A new therapeutic target? Circulation 109: 1580-1589, 2004.
2. Glenn DJ, Rahmutula D, Nishimoto M, Liang F and Gardner DG: Atrial natriuretic peptide suppresses endothelin gene expression and proliferation in cardiac fibroblasts through a GATA4-dependent mechanism. Cardiovasc Res 84: 209-217, 2009.
3. Eom GH and Kook H: Role of histone deacetylase 2 and its post-translational modifications in cardiac hypertrophy. BMB Rep 48: 131-138, 2015.
4. Glickman MH and Ciechanover A: The ubiquitin-proteasome proteolytic pathway: Destruction for the sake of construction. Physiol Rev 82: 373-428, 2002.
5. D'Ascenzi F, Pelliccia A, Corrado D, Cameli M, Curci V, Alvino F, Natali BM, Focardi M, Bonifazi M and Mondillo S: Right ventricular remodelling induced by exercise training in competitive athletes. Eur Heart J Cardiovasc Imaging 17: 301-307, 2016.
6. Bernardo BC, Weeks KL, Pretorius L and McMullen JR: Molecular distinction between physiological and pathological cardiac hypertrophy: Experimental findings and therapeutic strategies. Pharmacol Ther 128: 191-227, 2010.
7. Heineke J and Molkentin JD: Regulation of cardiac hypertrophy by intracellular signalling pathways. Nat Rev Mol Cell Biol 7: 589-600, 2006.
8. Sawyer DB, Siwik DA, Xiao L, Pimentel DR, Singh K and Colucci WS: Role of oxidative stress in myocardial hypertrophy and failure. J Mol Cell Cardiol 34: 379-388, 2002.
9. Fiorillo C, Nediani C, Ponziani V, Giannini L, Celli A, Nassi N, Formigli L, Perna AM and Nassi P: Cardiac volume overload rapidly induces oxidative stress-mediated myocyte apoptosis and hypertrophy. Biochim Biophys Acta 1741: 173-182, 2005.
10. Parsons JL and Chipman JK: The role of glutathione in DNA damage by potassium bromate in vitro. Mutagenesis 15: 311-316, 2000.
11. Watanabe S, Togashi S and Fukui T: Contribution of nitric oxide to potassium bromate-induced elevation of methaemoglobin concentration in mouse blood. Biol Pharm Bull 25: 1315-1319, 2002.
12. DeAngelo AB, George MH, Kilburn SR, Moore TM and Wolf DC: Carcinogenicity of potassium bromate administered in the drinking water to male B6C3F1 mice and F344/N rats. Toxicol Pathol 26: 587-594, 1998.
13. Kujawska M, Ignatowicz E, Ewertowska M, Adamska T, Markowski J and Jodynis-Liebert J: Attenuation of KBrO3-induced renal and hepatic toxicity by cloudy apple juice in rat. Phytother Res 27: 1214-1219, 2013.
14. Ishidate M Jr, Sofuni T, Yoshikawa K, Hayashi M, Nohmi T, Sawada M and Matsuoka A: Primary mutagenicity screening of food additives currently used in Japan. Food Chem Toxicol 22: 623-636, 1984.
15. Priscilla DH and Prince PS: Cardioprotective effect of gallic acid on cardiac troponin-T, cardiac marker enzymes, lipid peroxidation products and antioxidants in experimentally induced myocardial infarction in Wistar rats. Chem Biol Interact 179: 118-124, 2009.
16. Oseni OA, Ogunmoyole T and Idowu KA: Lipid profile and cardio-protective effects of aqueous extract of moringa oleifera (lam) leaf on bromate-induced cardiotoxicity on Wistar albino rats. Eur J Adv Res Biol Life Sci 3: 52-66, 2015.
17. Saad HB, Boudawara O, Hakim A and Amara IB: Preventive effect of vanillin on lipid peroxides andantioxidants in potassium bromate-inducedcardiotoxicity in adult mice: Biochemical andhistopathological evidences. J Pharmacognosy Phytochemistry 6: 1379-1383, 2017.
18. Khatua TN, Borkar RM, Mohammed SA, Dinda AK, Srinivas R and Banerjee SK: Novel sulfur metabolites of garlic attenuate cardiac hypertrophy and remodeling through induction of Na+/K+-ATPase Expression. Front Pharmacol 8: 18, 2017.

19. Chen ZC, Yu BC, Chen LJ, Cheng KC, Lin HJ and Cheng JT: Characterization of the mechanisms of the increase in PPARδ expression induced by digoxin in the heart using the H9c2 cell line. Br J Pharmacol 163: 390-398, 2011.
20. Zhu W, Zou Y, Shiojima I, Kudoh S, Aikawa R, Hayashi D, Mizukami M, Toko H, Shibasaki F, Yazaki Y, *et al*: Ca2+/calmodulin-dependent kinase II and calcineurin play critical roles in endothelin-1-induced cardiomyocyte hypertrophy. J Biol Chem 275: 15239-15245, 2000.
21. Asadi F, Razmi A, Dehpour AR and Shafiei M: Tropisetron inhibits high glucose-induced calcineurin/NFAT hypertrophic pathway in H9c2 myocardial cells. J Pharm Pharmacol 68: 485-493, 2016.
22. Han YH and Park WH: Tiron, a ROS scavenger, protects human lung cancer Calu-6 cells against antimycin A-induced cell death. Oncol Rep 21: 253-261, 2009.
23. Oyewole AO and Birch-Machin MA: Mitochondria-targeted antioxidants. FASEB J 29: 4766-4771, 2015.
24. Lo SH, Hsu CT, Niu HS, Niu CS, Cheng JT and Chen ZC: Ginsenoside Rh2 improves cardiac fibrosis via PPARdelta-STAT3 signaling in type 1-like diabetic rats. Int J Mol Sci 18: pii: E1364, 2017.
25. Li CJ, Lin L, Li H and Yu DM: Cardiac fibrosis and dysfunction in experimental diabetic cardiomyopathy are ameliorated by alpha-lipoic acid. Cardiovasc Diabetol 11: 73, 2012.
26. Lo SH, Cheng KC, Li YX, Chang CH, Cheng JT and Lee KS: Development of betulinic acid as an agonist of TGR5 receptor using a new in vitro assay. Drug Des Devel Ther 10: 2669-2676, 2016.
27. Livak KJ and Schmittgen TD: Analysis of relative gene expression data using real-time quantitative PCR and the 2(-Delta Delta C(T)) method. Methods 25: 402-408, 2001.
28. Wang CM, Hsu CT, Niu HS, Chang CH, Cheng JT and Shieh JM: Lung damage induced by hyperglycemia in diabetic rats: The role of signal transducer and activator of transcription 3 (STAT3). J Diabetes Complications 30: 1426-1433, 2016.
29. Scudiero DA, Shoemaker RH, Paull KD, Monks A, Tierney S, Nofziger TH, Currens MJ, Seniff D and Boyd MR: Evaluation of a soluble tetrazolium/formazan assay for cell growth and drug sensitivity in culture using human and other tumor cell lines. Cancer Res 48: 4827-4833, 1988.
30. Calastretti A, Gatti G, Quaresmini C and Bevilacqua A: Down-modulation of Bcl-2 sensitizes PTEN-mutated prostate cancer cells to starvation and taxanes. Prostate 74: 1411-1422, 2014.
31. Fiedler B and Wollert KC: Interference of antihypertrophic molecules and signaling pathways with the Ca2+-calcineurin-NFAT cascade in cardiac myocytes. Cardiovasc Res 63: 450-457, 2004.
32. Kwon SH, Pimentel DR, Remondino A, Sawyer DB and Colucci WS: H(2)O(2) regulates cardiac myocyte phenotype via concentration-dependent activation of distinct kinase pathways. J Mol Cell Cardiol 35: 615-621, 2003.
33. El-Deeb MEE and Abd-El-Hafez AAA: Can vitamin C affect the $KBrO_3$ induced oxidative stress on left ventricular myocardium of adult male albino rats? A histological and immunohistochemical study. J Microsc Ultrastruct 3: 120-136, 2015.
34. Sagnella GA: Measurement and significance of circulating natriuretic peptides in cardiovascular disease. Clin Sci (Lond) 95: 519-529, 1998.
35. Liu N, Chai R, Liu B, Zhang Z, Zhang S, Zhang J, Liao Y, Cai J, Xia X, Li A, *et al*: Ubiquitin-specific protease 14 regulates cardiac hypertrophy progression by increasing GSK-3β phosphorylation. Biochem Biophys Res Commun 478: 1236-1241, 2016.
36. Waspe LE, Ordahl CP and Simpson PC: The cardiac beta-myosin heavy chain isogene is induced selectively in alpha 1-adrenergic receptor-stimulated hypertrophy of cultured rat heart myocytes. J Clin Invest 85: 1206-1214, 1990.
37. Younce CW, Wang K and Kolattukudy PE: Hyperglycaemia-induced cardiomyocyte death is mediated via MCP-1 production and induction of a novel zinc-finger protein MCPIP. Cardiovasc Res 87: 665-674, 2010.
38. Zuo L, Youtz DJ and Wold LE: Particulate matter exposure exacerbates high glucose-induced cardiomyocyte dysfunction through ROS generation. PLoS One 6: e23116, 2011.
39. Goldhaber JI: Free radicals enhance Na+/Ca2+ exchange in ventricular myocytes. Am J Physiol 271: H823-H833, 1996.
40. Huynh K, Kiriazis H, Du XJ, Love JE, Gray SP, Jandeleit-Dahm KA, McMullen JR and Ritchie RH: Targeting the upregulation of reactive oxygen species subsequent to hyperglycemia prevents type 1 diabetic cardiomyopathy in mice. Free Radic Biol Med 60: 307-317, 2013.
41. Jiang P, Zhang D, Qiu H, Yi X, Zhang Y, Cao Y, Zhao B, Xia Z and Wang C: Tiron ameliorates high glucose-induced cardiac myocyte apoptosis by PKCδ-dependent inhibition of osteopontin. Clin Exp Pharmacol Physiol 44: 760-770, 2017.
42. Khan S, Zhang D, Zhang Y, Li M and Wang C: Wogonin attenuates diabetic cardiomyopathy through its anti-inflammatory and anti-oxidative properties. Mol Cell Endocrinol 428: 101-108, 2016.
43. Schröder E and Eaton P: Hydrogen peroxide as an endogenous mediator and exogenous tool in cardiovascular research: Issues and considerations. Curr Opin Pharmacol 8: 153-159, 2008.
44. Park JH, Lee JH and Park JW: Attenuated SAG expression exacerbates 4-hydroxy-2-nonenal-induced apoptosis and hypertrophy of H9c2 cardiomyocytes. Free Radic Res 49: 962-972, 2015.
45. Mishra S and Chatterjee S: Lactosylceramide promotes hypertrophy through ROS generation and activation of ERK1/2 in cardiomyocytes. Glycobiology 24: 518-531, 2014.
46. Abdel Gadir EH, Abdel Gadir WS and Adam SEI: Effects of various levels of dietary potassium bromate on wistar rats. J Pharmacol Toxicol 2: 672-676, 2007.
47. Khan MR, Haroon J, Ali Khan R, Bokhari J, Shabbir M and Rashid U: Prevention of $KBrO_3$-induced cardiotoxicity by Sonchus asper in rat. J Med Plants Res 5: 2514-2520, 2011.
48. Kumar S and Pankaj P: Accidental potassium bromate poisoning in nine adults. J Indian Acad Forensic Med 34: 364-366, 2012.